Vol 18 No 2, p 179-184

COMPUTED TOMOGRAPHY AND CROSS-SECTIONAL ANATOMY OF THE THORAX OF TWO NEWBORN DROMEDARY CAMELS

A. Arencibia, M.A. Rivero, G. Ramírez-Zarzosa, D. Blanco, M. Morales[2] and J.M. Vázquez[1]
Department of Morphology, Veterinary Faculty, University of Las Palmas de Gran Canaria, Arucas 35413, Spain
Department of Anatomy[1], Veterinary Faculty, University of Murcia, Murcia 30100, Spain
Department of Animal Pathology[2], Veterinary Faculty, University of Las Palmas de Gran Canaria, Arucas 35413, Spain

ABSTRACT

The objective of this study is to provide an overview of the normal cross-sectional anatomy of the camel thorax using computed tomography (CT) images in 2 cadaver newborn dromedary camels. The camels were supported in sternal recumbency and CT scan was performed from the brachiocephalic trunk to the heart apex, with 3 mm slice thickness. A soft-tissue and lung windows settings were used. At the end of the CT study, cross-sections of the camel thorax were obtained as anatomical reference. Clinically relevant anatomical structures were identified and labelled in the CT images and cross-sections. Gross anatomical images provided an excellent anatomical details to characterise the CT anatomy of the camel thorax. The information presented in this study should serve as an initial reference to evaluate CT images of the camel thorax and assist in the interpretation of lesions in this region.

Key words: Computed tomography, cross-sectional anatomy, dromedary camel, thorax

Computed tomography (CT) is a modern medical diagnostic imaging technique. It has a superior spatial resolution and good discrimination between bone and soft tissue compared with other conventional diagnostic techniques, such as radiography or thoracic ultrasound. Several studies have demonstrated the clinical value of CT in veterinary medicine. In small animals, the evolution of CT as a diagnostic technique has become a useful diagnostic tool for the thorax anatomical studies (Cardoso *et al,* 2007; Feeney *et al,* 1991; Rivero *et al,* 2005) and for evaluating intrathoracic diseases (Henninger, 2003; Spann *et al,* 1998). However, reports of CT in the goat and the sheep have been limited to the head (Arencibia *et al,* 1997; Gonzalo Orden *et al,* 2000; Warderman and Van Weeren, 1996) and thorax (Alsafy 2008; Braun *et al,* 2009; Smallwood and Healey, 1982; Staffieri *et al,* 2010).

In camel medicine, due to its high cost and limited access to scanners, CT has been used only sparingly for diagnostic and research on alpacas (Adolf *et al,* 2001; Amory *et al,* 2010) and llamas (Boon *et al,* 1994; Byers *et al,* 2007; Hathcock *et al,* 1995; Step *et al,* 2003; Van Hoogmoed *et al,* 1998). South American camelids are becoming increasingly popular in several countries and they are kept as pets (Margiocco *et al,* 2009). Knowledge of the CT appearance of the normal camel thorax is necessary for the evaluation of cardiac chamber size (e.g. cardiomyopathiel) and cardiopulmonary vascular diseases (e.g. congenital aberrant vessels, cardiac or pulmonary vascular stenosis, thrombi). The purpose of this report is to provide an overview of normal cross-sectional anatomy of the newborn dromedary camel thorax structures using CT images and anatomical cross-sections.

Materials and Methods

Animals

Two newborn dromedary camels, ranged 35-45 kg weight, dead for medical reasons unrelated to thoracic cavity diseases were used for this study. The camels belonged to a camel farm located in Fataga, Gran Canaria, Canary Islands, Spain.

CT scan technique

CT imaging was performed at the Radiodiagnostic Service of the Hospital Universitario Insular of Las Palmas de Gran Canaria, Spain, with a Toshiba 600 HQ scanner. Throughout the procedure the animals were positioned in ventral recumbency during scanning time. Transverse CT images from

SEND REPRINT REQUEST TO A. ARENCIBIA email: aarencibia@dmor.ulpgc.es

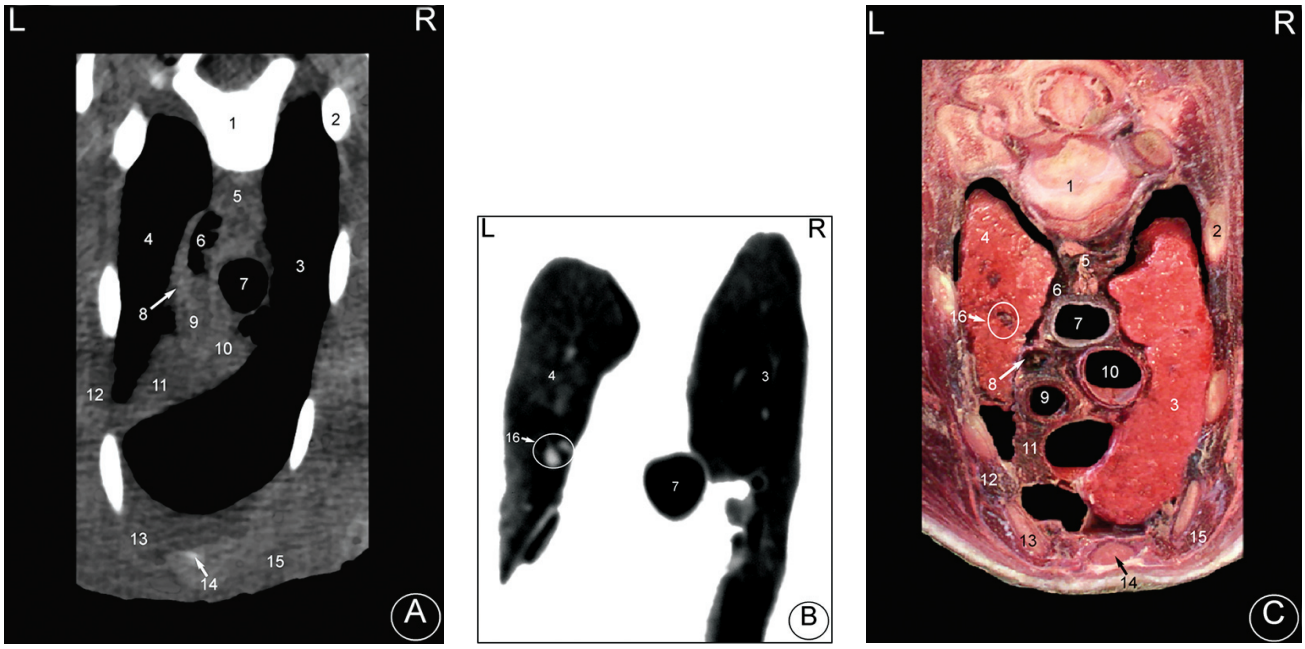

Fig 1. Transverse images at the level of the brachiocephalic trunk. (A) CT-soft tissue window image, (B) CT-lung window image and (C) Anatomical cross-section. L: Left; R: Right.

1. Body of thoracic vertebra; 2. Rib: costal bone; 3. Right cranial lung lobe; 4. Left cranial lung lobe; 5. Longus colli muscle; 6. Oesophagus: thoracic part; 7. Trachea: thoracic part; 8. Left subclavian artery; 9. Brachiocephalic trunk; 10. Cranial vena cava; 11. Thymus; 12. Thoracic walls muscles; 13. Rib: costal cartilage; 14. Sternum; 15. Pectoral muscles; 16. Left lobar pulmonary vein, the lobar arterial branch and the lobar bronchus.

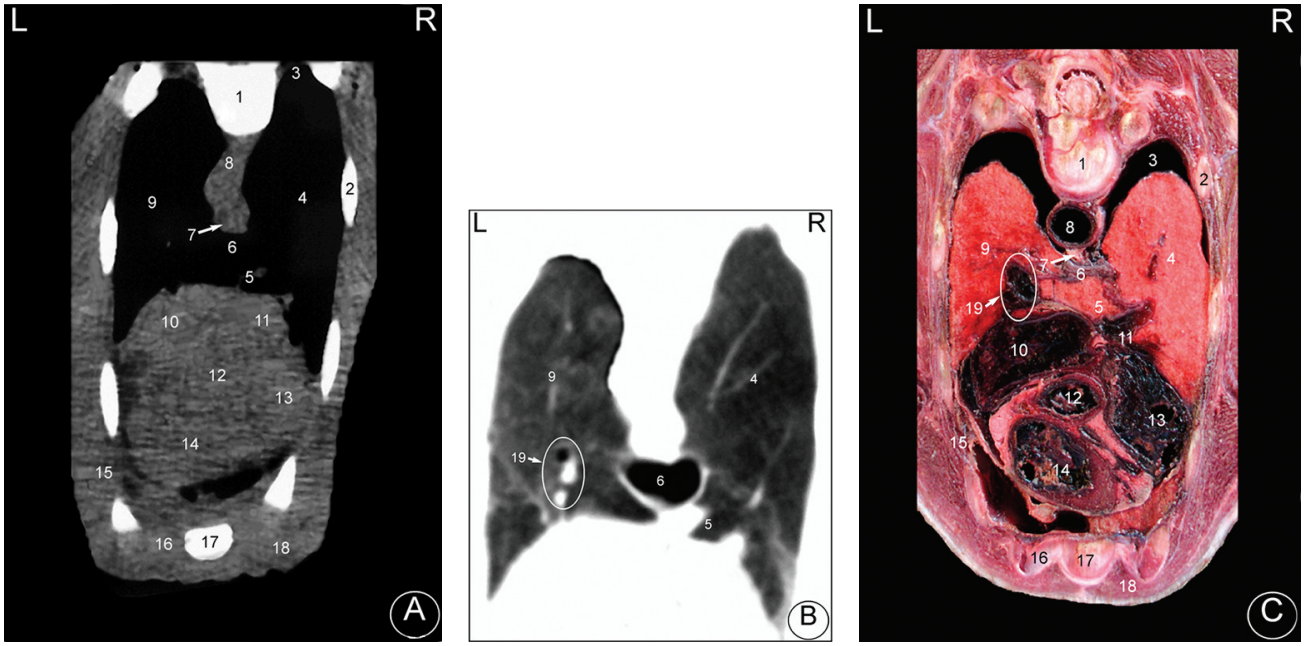

Fig 2. Transverse images at the level of the tracheal carina. (A) CT-soft tissue window image, (B) CT-lung window image and (C) Anatomical cross-section. L: Left; R: Right.

1. Body of thoracic vertebra; 2. Rib: costal bone; 3. Pleural cavity; 4. Right cranial lung lobe; 5. Accessory lung lobe; 6. Tracheal carina; 7. Oesophagus: thoracic part; 8. Descending aorta; 9. Left cranial lung lobe; 10. Left atrium; 11. Right atrium; 12. Ascending aorta; 13. Right ventricle; 14. Left ventricle; 15. Thoracic walls muscles; 16. Rib: costal cartilage; 17. Sternum; 18. Pectoral muscles. 19. Left lobar pulmonary vein, the lobar arterial branch and the lobar bronchus.

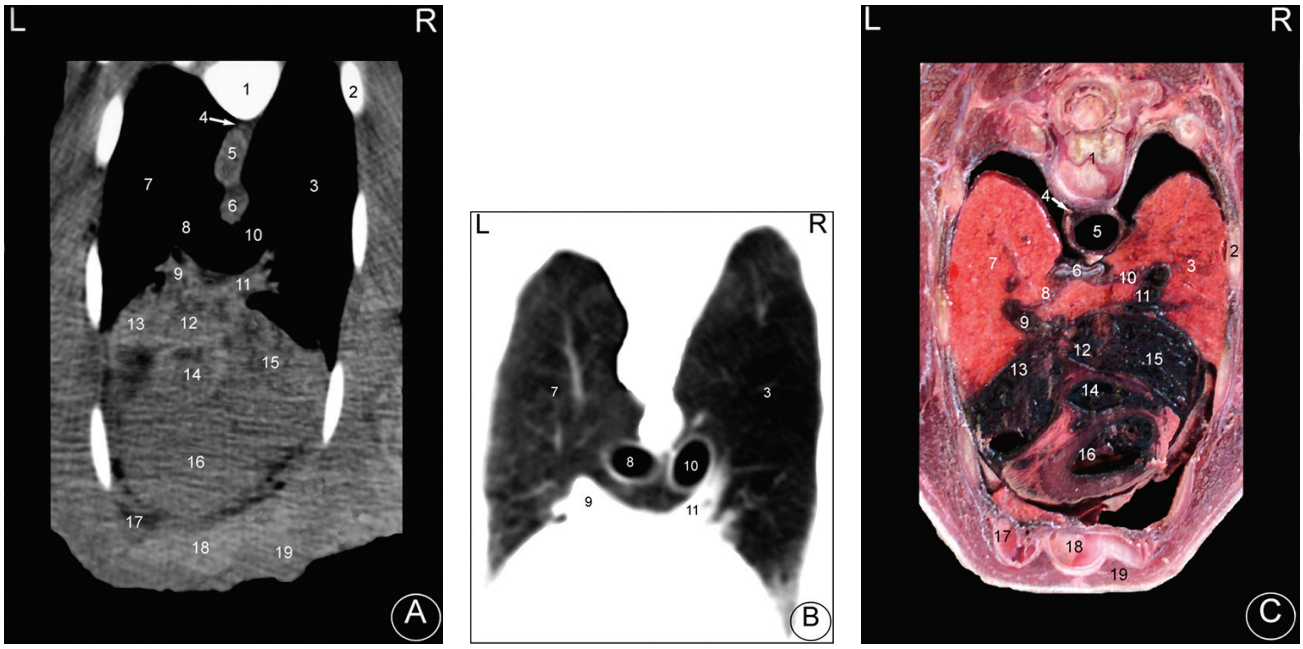

Fig 3. Transverse images at the level of the pulmonary trunk bifurcation into the right and left pulmonary arteries. (A) CT-soft tissue window image, (B) CT-lung window image and (C) Anatomical cross-section. L: Left; R: Right.

1. Body of thoracic vertebra; 2. Rib: costal bone; 3. Right cranial and middle lung lobes; 4. Left azygous vein; 5. Descending aorta; 6. Oesophagus: thoracic part; 7. Left cranial lung lobe; 8. Left principal bronchus; 9. Left pulmonary artery; 10. Right principal bronchus; 11. Right pulmonary artery; 12. Pulmonary trunk; 13. Left atrium; 14. Aortic bulb; 15. Right atrium; 16. Right ventricle; 17. Rib: costal cartilage; 18. Sternum; 19. Pectoral muscles.

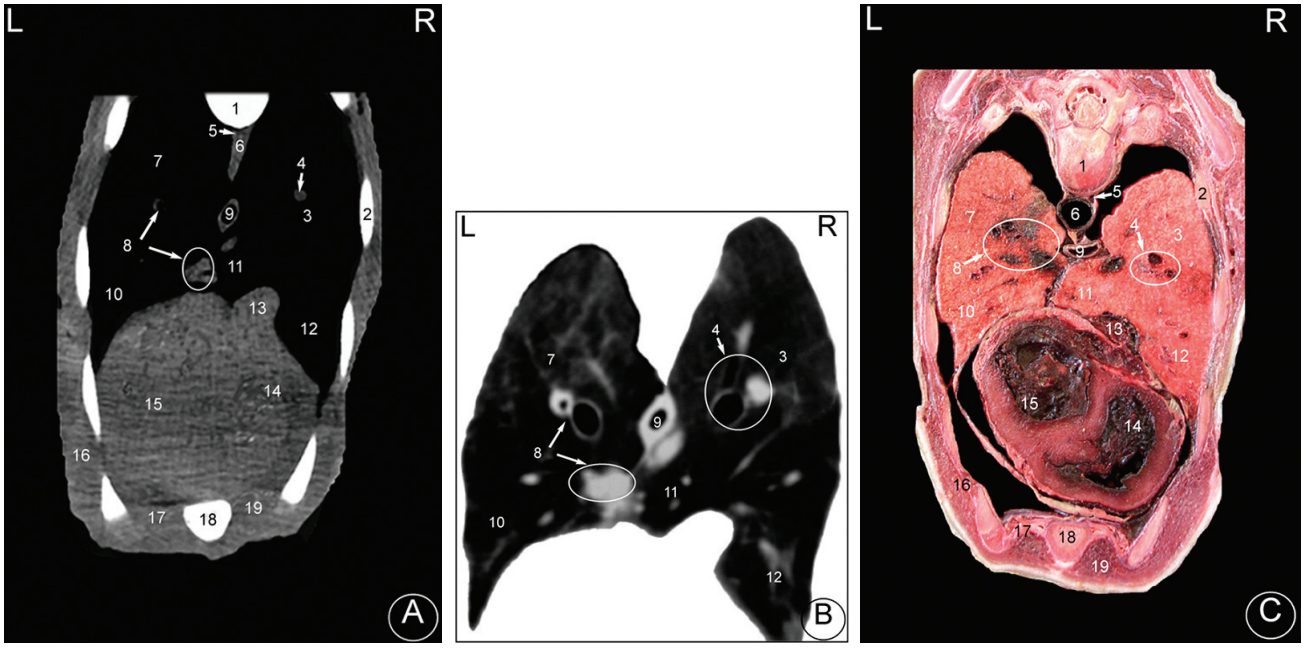

Fig 4. Transverse images at the level of the 5th thoracic vertebra. (A) CT-soft tissue window image, (B) CT-lung window image and (C) Anatomical cross-section. L: Left; R: Right.

1. Body of thoracic vertebra; 2. Rib: costal bone; 3. Right cranial and middle lung lobes; 4. Right lobar pulmonary vein, the lobar arterial branch and the lobar bronchus; 5. Left azygous vein; 6. Descending aorta; 7. Left cranial lung lobe; 8. Left lobar pulmonary vein, the lobar arterial branch and the lobar bronchus; 9. Oesophagus: thoracic part; 10. Left caudal lung lobe; 11. Accessory lung lobe; 12. Right caudal lung lobe; 13. Caudal vena cava; 14. Right ventricle; 15. Left ventricle; 16. Thoracic walls muscles; 17. Rib: costal cartilage; 18. Sternum; 19. Pectoral muscles.

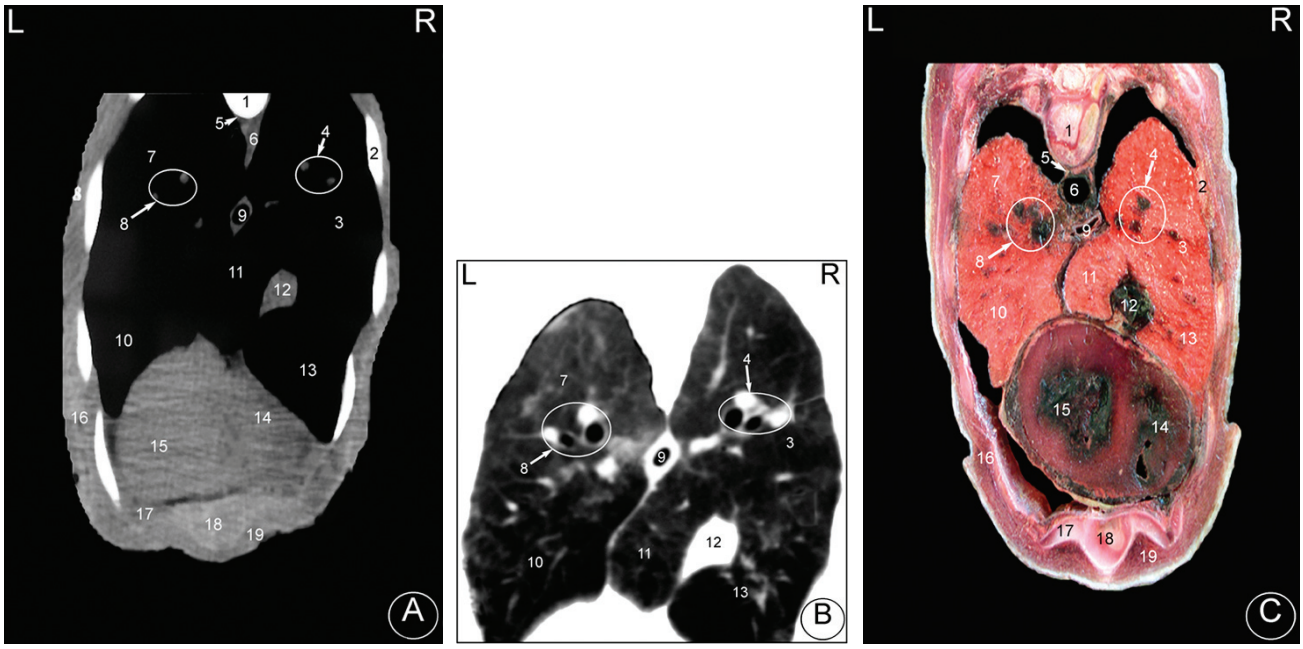

Fig 5. Transverse images at the level of the heart apex. (A) CT-soft tissue window image, (B) CT-lung window image and (C) Anatomical cross-section. L: Left; R: Right

1. Body of thoracic vertebra; 2. Rib: costal bone; 3. Right cranial and middle lung lobes; 4. Right lobar pulmonary vein, the lobar arterial branch and the lobar bronchus; 5. Left azygous vein; 6. Descending aorta; 7. Left cranial lung lobe; 8. Left lobar pulmonary vein, the lobar arterial branch and the lobar bronchus; 9. Oesophagus: thoracic part; 10. Left caudal lung lobe; 11. Accessory lung lobe; 12. Caudal vena cava; 13. Right caudal lung lobe; 14. Right ventricle; 15. Left ventricle and heart apex; 16. Thoracic walls muscles; 17. Rib: costal cartilage; 18. Sternum; 19. Pectoral muscles.

the brachiocephalic trunk to the apex of heart were obtained using the following parameters: caudal vision of image (V.V.F.), 3 s exposure time, 120 kV, 130 mA and 3 mm slice thickness and 3 mm image spacing. Best image quality for soft tissue was obtained by adjusting window widths and window levels. For visualising soft tissue thoracic structures, a soft-tissue window setting (window width, 350; window level, 83) was used. For pulmonary parenchyma and associated structures a lung window setting (window width, 1200; window level, -600) was used.

Anatomical evaluation

At the end of the CT study, the cadavers were frozen and sectioned using an electric bandsaw at the positions which matched the CT-images as closely as possible. CT images were compared to the corresponding cross-sections and with anatomy books (Schaller, 2007; Smuts and Bezuidenhout, 1987), to identify the normal CT anatomy of the heart, lungs and associated structures of the camel thorax. Some formations show in the anatomical sections could not be seen on CT images and *vice versa*. Several thoracic vascular structures were labelled according to an internationally accepted nomenclature (Schaller, 2007).

Results

In this study, 5 figures corresponding to the CT images obtained with the soft tissue and lung windows settings along with anatomic cross-sections of camel thorax are presented (Figs 1-5). All the figures are shown in a cranial to caudal progression from the level of the brachiocephalic trunk (Fig 1) to the apex of the heart (Fig 5) and viewed from the caudal view.

In the CT-soft tissue window images, the bones of the thorax (thoracic vertebrae, ribs and sternum) could be visualised because of the high CT density. The costal cartilages and the costo-vertebral, costo-chondral and sterno-costal joints had a low density. Muscular tissues (pectoral and thoracic walls muscles) had an intermediate CT density and appeared grey. Skin, subcutaneous tissue, thymus and fat (pericardial and mediastinal) had a low-intermediate density and were easily differentiated because of their CT density compared to adjacent anatomical structures, such as the respiratory system and oesophagus. Because of the air in the lumen, the trachea, the parenchyma of the lungs, the main bronchi., the lobular bronchi. and oesophagus had negligible CT-tissue density and appeared black. However, vascular and bronchial

wall were identified by their intermediate CT density. The heart cavities (anta and ventricles) and associated blood vessels (cranial and caudal cava veins, left azygous vein, ascending aorta, brachiocephalic trunk, left subclavian artery, descending aorta and pulmonary vessels) were identified by their intermediate attenuation in the CT images. Inside the pulmonary parenchyma, the lobar pulmonary veins and the lobar branches of the pulmonary arteries were not very evident.

In the CT-lung window images, the degree of hypoattenuation of the lungs was not so intense. It allowed a better definition of the pulmonary lobes and a better tomographical definition of the trachea, main bronchi and lobar bronchi because all these structures presented a higher radiotransparency than the lung. At the level of the pulmonary parenchyma, the vascular structures were better defined compared to soft-tissue window. In this sense, it was visualised that the triad comprises the lobar pulmonary vein, the lobar arterial branch and the lobar bronchus. The pleural cavity presented a light tomographic sign, not being observed in the soft tissue window. With the lung window images, it was possible to recognise at the level of the tracheal bifurcation, the tracheal carina, which was not observed with the soft-tissue window.

Discussion

In veterinary medicine, radiography and ultrasound are the imaging modalities of choice for camelid thorax (Cebra *et al,* 1998; Gall *et al,* 2006; Margiocco *et al,* 2009; Mattoon *et al,* 2001), although it is increasingly recognised that CT can provide information that cannot be obtained by other means, because of its capacity to discriminate the different tissues (Alsafy, 2008; Feeney *et al,* 1991; Rivero *et al,* 2005). CT thorax scans provide considerable advantages over other diagnostic imaging techniques. Structures are viewed without superimposition; including additional cross-sectional anatomical information, superior contrast resolution of bones and soft-tissues (Alsafy, 2008; Feeney *et al,* 1991; Rivero *et al,* 2005) and a more sensitive technique to diagnosis thoracic diseases (Adolf *et al,* 2001; Amory *et al,* 2010). However, there are some disadvantages of the CT technique compared with conventional radiography and ultrasound. These include high cost, low accessibility and logistic problems of acquiring CT images in large animals, and besides, the need for general anaesthesia for the CT examination.

In CT technique, choosing the appropriate CT window, also allows modification of the attenuation degree, inside some limits, to improve the definition of certain structures (Cardoso *et al,* 2007). This fact should be considered when the organs of the thorax are analysed, because of the wide range of CT numbers (HU) that present their tissues (Cardoso *et al,* 2007; Feeney *et al,* 1991). However, the heart chambers are not visible with the same precision as using ultrasound, where these cameras can seen internally (Margiocco *et al,* 2009); CT only to distinguish the outline of the chambers when there are different degrees of attenuation between the tissues that form the periphery of the anatomical structures, such as fat.

CT scans resulting from these techniques require a thorough knowledge of the regional cross-sectional anatomy (Alsafy, 2008; Hathcock *et al,* 1995; Rivero *et al,* 2005; Smallwood and Healey, 1982). In our study, CT images of the camel thorax had provided details of anatomy, clinically relevant, a good correlation with thoracic sections and discrimination of both soft and mineralised tissues. The sectional anatomy of the thoracic cavity in the camel allowed a correct morphologic and topographic evaluation of the anatomical structures, and it is a helpful tool for the identification of the CT images. In this sense, we considered it quite useful to be able to establish some references on camel thoracic topography, mainly from the vascular system in order to scan only selected parts during a clinical or experimental approach.

With developing technology, CT imaging will soon become more readily available for camel diagnostic imaging. Diagnoses of diseases, such as trauma, neoplasms, infection, inflammations, and others involving the thoracic cavity can be improved in camel using CT imaging (Henninger, 2003; McKenzie *et al,* 2010; Spann *et al,* 1998).

In conclusion, CT provided an excellent anatomical details to characterise the CT anatomy of the camel thorax. The information presented in this study should serve as an initial reference to anatomic evaluation of camel thorax CT images and to assist interpretation of lesions of this region.

References

Adolf J, Dykes N, Semevolos S and Divers T (2001). The diagnosis and treatment of a thoracic abscess in an alpaca. Australian Veterinary Journal 79:675-679.

Alsafy MA (2008). Computed tomography and cross-sectional anatomy of the thorax of goat. Small Ruminant Research 79:158-166.

Amory JT, Jones JC, Crisman MV, Zimmerman K, Tyson AR 3rd, Larson MM, Saunders GK and O'Rourke LG (2010). Imaging diagnosis-Dorsal mediastinal T-cell lymphoma

in an alpaca. Veterinary Radiology and Ultrasound 51:311-312.

Arencibia A, Vázquez JM, Ramírez JA, Sandoval JA, Ramírez G and Sosa C (1997). Anatomy of the cranioencephalic structures of the goat (*Capra hircus L.*) by imaging techniques: a computerised tomographic study. Anatomia Histologia Embryologia 26:161-164.

Boon JA, Knight AP and Moore DH (1994). Llama cardiology. Veterinary Clinics of North America Food Animal Practice 10:353-370.

Braun U, Steininger K, Irmer M, Hagen R, Ohlerth S, Ruhl S and Ossent P (2009). Ultrasonographic and computed tomographic findings in a goat with mediastinal lymphocytic thymoma. Schweiz Arch Tierheilkd 151:332-335.

Byers SR, Parish SM, Holmes SP, Donahoe SL and Barrington GM (2007) A fungal granuloma of the frontal sinus in a llama. Canadian Veterinary Journal 48:939-941.

Cardoso L, Gil F, Ramírez G, Teixeira MA, Agut A, Rivero MA, Arencibia A and Vázquez JM (2007). Computed tomography (CT) of the lungs of the dog using a helical CT scanner, intravenous iodine contrast medium and different CT windows. Anatomia Histologia Embryologia 36:328-331.

Cebra ML, Cebra CK, Garry FB, Boon JA and Orton EC (1998). Atrioventricular septal defects in 3 llamas (*Lama lama*). Journal of Zoo and Wildlife Medicine 29:225-227.

Feeney D, Fletcher T and Hardy R (1991). Atlas of Correlative Imaging Anatomy of the Normal Dog. Ultrasound and computed tomography. WB Saunders, Philadelphia.

Gall DA, Zekas LJ, Van Metre D and Holt T (2006). Imaging diagnosis-pulmonary metastases in new world camelids. Veterinary Radiology and Ultrasound 47:571-573.

Gonzalo-Orden JM, Altonaga JR, Díez A, Gonzalo JM and Orden MA (2000). Correlation between MRI, computed tomographic findings and clinical signs in a case of ovine coenurosis. Veterinary Record 146:352-353.

Hathcock JT, Pugh DG, Cartee RE and Hammond L (1995). Computed tomography of the llama head: technique and normal anatomy. Veterinary Radiology and Ultrasound 36:290-296.

Henninger W (2003). Use of computed tomography in the diseased feline thorax. The Journal of Small Animal Practice 44:56-64.

Margiocco ML, Scansen BA and Bonagura JD (2009). Camelid cardiology. Veterinary Clinics of North America Food Animal Practice 25:423-454.

Mattoon JS, Gerros TC and Brimacombe M (2001). Thoracic radiographic appearance in the normal llama. Veterinary Radiology and Ultrasound 42:28-37.

McKenzie EC, Seguin B, Cebra CK, Margiocco ML, Anderson DE and Löhr CV (2010). Oesophageal dysfunction in four alpaca crias and a llama cria with vascular ring anomalies. Journal of the American Veterinary Medical Association 237:311-316.

Rivero MA, Ramírez JA, Vázquez JM, Gil F, Ramírez G and Arencibia A (2005). Normal anatomical imaging of the thorax in three dogs: computed tomography and macroscopic cross sections with vascular injection. Anatomia Histologia Embryologia 34:215-219.

Schaller O (2007). Illustrated Veterinary Anatomical Nomenclature. 2nd Ed. Sttutgart: Ferdinand Enke Verlag.

Smuts MM and Bezuidenhout AJ (1987). Anatomy of Dromedary. Clarendon Press, Oxford.

Smallwood JE and Healey WV (1982). Computed tomography of the thorax of the adult Nubian goat. Veterinary Radiology 23:135-143.

Spann DR, Sellon RK, Thrall DE, Bostian AE and Boston GT (1998). Computed tomographic diagnosis: use of computed tomography to distinguish a pulmonary mass from alveolar disease. Veterinary Radiology and Ultrasound 39:532-535.

Staffieri F, Driessen B, Monte VD, Grasso S and Crovace A (2010). Effects of positive end-expiratory pressure on anaesthesia-induced atelectasis and gas exchange in anaesthetised and mechanically ventilated sheep. American Journal of Veterinary Research 71:867-74.

Step DL, Ritchey JW, Drost WT and Bahr RJ (2003). Ameloblastic odontoma in the mandible of a llama. Canadian Veterinary Journal 44:824-827.

Van Hoogmoed L, Roberts G, Snyder JR, Yarbrough T and Harmon F (1998). Use of computed tomography to evaluate the intestinal tract of adult llamas. Veterinary Radiology and Ultrasound 39:117-122.

Warderman EP and Van Weeren PR (1996). Computed tomography and treatment of chronic temporo-mandibular joint arthritis in a sheep. Vet Quaterly 18:94-96.